Modes on a bent optical waveguide

S.J. Garth, PhD

Indexing terms: Waveguides and waveguiding components, Perturbation theory, Electromagnetic theory, Optical fibres

Abstract: The scalar propagation characteristics of a bent optical waveguide are investigated. Using a first-order perturbation theory, analytic solutions for the fields and propagation constants of any mode, of either even or odd symmetry, are obtained. The bend breaks the degeneracy of the higher-order scalar propagation constants, and the modes become truly polarised with fixed field directions in the fibre. A more exact analysis is used to investigate the modal properties of the bent slab waveguide, and an expression for the radiation point, which is the point in the cladding at which the field becomes radiative, is derived. Using a Gaussian function to approximate the fields, the range of validity of the perturbation expansion is discussed.

1 Introduction

The use of optical waveguides in communication systems or as optical sensing devices requires an understanding of their modal properties. In particular, the effect on these properties when the waveguide is perturbed in some manner must be analysed so that it can either be eliminated or incorporated into the design of the optical system. In this paper we examine changes to the propagation characteristics occurring when optical waveguides are bent.

The literature concerned with bends and microbends on waveguides is extensive, but in general these studies have dealt with radiation losses [1–3]. We will not be concerned with loss here, although the perturbed fields derived in Section 4.1 may be used to obtain more accurate bending-loss results, as reported previously [4–6].

When an optical fibre or waveguide is bent it is well known that the modal field will shift towards the outer core/cladding boundary as the bend radius decreases, but the effect on the modal propagation constants, which dictate the dispersion and group-delay properties of the fibre, is not widely understood.

We present simple formulas describing the perturbations to the fields and propagation constants of any mode, of either even or odd symmetry. We show that bending the waveguide causes the higher-order scalar propagation constants to become nondegenerate. The mode splits into odd and even symmetries which propagate through the fibre with different polarisation directions and different group delays.

Paper 5495J (E13), first received 19th November 1986 and in revised form 9th February 1987

The author is with the Department of Mathematics, University College, Australian Defence Force Academy, Northcott Drive, Campbell, ACT, 2600, Australia

We consider weakly guiding waveguides, in which the refractive index in the core n_{co} and refractive index in the cladding n_{cl} are approximately equal, so that the index difference $\Delta \equiv (n_{co} - n_{cl})/n_{co} \simeq 0$. With this approximation the problem simplifies because the polarisation properties of the modes can be treated separately. The modes are treated as scalar modes multiplied by a polarisation term.

Let us first consider these polarisation effects. The commonly used linearly polarised (LP) modes [7, 8] are nearly correct for a straight fibre and polarisation corrections are given in Reference 9. In a straight fibre with a circularly symmetric core there are no uniquely defined polarisation axes. However, in a bent fibre, two definite axes are defined and the theory in Reference 9 shows that the modes will become truly linearly polarised — they will have fixed field directions in the fibre and maintain their initial state of polarisation. In Appendix 10 we give a quantitative analysis of the criteria for modes to be linearly polarised on a bent fibre. Thus our modes will consist of a scalar form multiplied by an appropriate polarisation unit vector.

In this paper we deal with the splitting of the degeneracy of the $l \geqslant 1$ scalar modes. The difference in propagation constants with respect to polarisation directions, i.e. birefringence, is not addressed here. These polarisation effects are small, and other mechanisms of birefringence, such as stress and elasto-optic effects, will dominate [10].

The scalar modes have fields and propagation constants that satisfy the scalar wave equation. For the higher-order modes of a straight, circularly symmetric fibre there are two solutions to this equation representing an even mode and an odd mode, with the propagation constant being equal for both symmetries. If the symmetry of the waveguide is disturbed, by having a noncircular cross-section for example [9], the degeneracy of the higher-order modes is broken and the propagation constants are different for the two symmetries.

We show that bending the fibre breaks the degeneracy of the scalar $l \geqslant 1$ modes. The propagation constant dictates the modal group delay of the waveguide, and thus the higher-order modes will separate as they propagate along the fibre with fixed orthogonal polarisation directions.

After deriving the field equations, a perturbation analysis is employed where the fields and propagation constants of the bent fibre are expanded in an ascending series of (ρ/a), where ρ is the waveguide radius and a is the bending radius. The first term in this series is the unperturbed or straight-waveguide solution. Each term in the series for the fields decays quickly to zero in the cladding, regardless of the magnitude of the bending radius. However, physically, modes become radiative when the radius is small enough, so that the perturbation solutions will only be accurate close to and within the core region.

The case of the step-index slab waveguide is examined, and more physical solutions, in which the field will no longer be bound for small bend radius, are presented. We determine the radiation point, which is the distance from the waveguide where the phase velocities of the propagating mode reaches the local speed of light and the field becomes radiative.

An analysis of the step-index optical fibre is then presented, where the solution of the fields and propagation constants of the $l = 0$ and $l = 1$ modes are derived. To first order, the propagation constant of the $l = 1$ mode becomes nondegenerate. Numerical results are presented for the clad power-law profile, and we suggest a nonlinear optics experiment as a way to measure the mode splitting. Finally, by using Gaussian approximations to describe the fields of the bent fibre the validity of the perturbation expansion is discussed.

Theoretical research on modal fields in a bent waveguide have been widely performed. The perturbation expansion used here has been used to analyse the fields and propagation constants of a single- and multilayered slab waveguide [11, 12]. Analytic solutions for the fields in a bent step-index fibre have been obtained using a first-order perturbation theory to the vector wave equation [13, 14], but the solutions are complicated. Experimental confirmation of the field shift in a bent fibre [15, 16] have been reported, and the use of a Gaussian field approximation to explain this shift has been used [17].

2 Field equations

The electric field of the guided mode is assumed to be linearly polarised, as vector or polarisation corrections are neglected and the 'weak-guidance' approximation is used [7, 8]. To derive the field equations, the wave equation is written in a cylindrical coordinate system ($\bar{X}$, $\bar{Y}$, $\bar{Z}$) or ($\bar{R}$, θ, $\bar{Y}$) with origin at the centre of curvature, as shown in Fig. 1. If we consider a $\bar{Y}$-polarised electric field

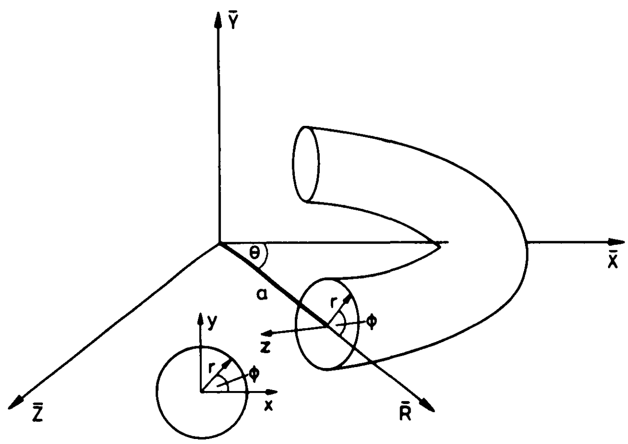

Fig. 1 *Cylindrical coordinate system ($\bar{R}$, θ, $\bar{Y}$) and local coordinate system (r, ϕ, z) of the bent fibre*

the scalar wave equation is

$$\left\{\frac{\partial^2}{\partial \bar{R}^2} + \frac{1}{\bar{R}}\frac{\partial}{\partial \bar{R}} + \frac{1}{\bar{R}^2}\frac{\partial^2}{\partial \theta^2} + \frac{\partial^2}{\partial \bar{Y}^2} + k^2 n^2\right\} E_{\bar{Y}} = 0$$

For a wave propagating along the θ- or z-axis, the wave equation can be converted to the local coordinate system (r, ϕ, z) where the following geometric relations are used:

$$\bar{R} = a + r\cos\phi$$

$$\theta = z/a$$

$$\bar{Y} = r\sin\theta$$

where a is the constant radius of curvature. The result of this transformation is

$$\left\{\frac{\partial^2}{\partial r^2} + \frac{1}{r}\frac{\partial}{\partial r} + \frac{1}{r^2}\frac{\partial^2}{\partial \phi^2} + k^2 n^2\right\} E + \left(1 + \frac{r}{a}\cos\phi\right)^{-2}\left\{\frac{1}{4a^2} - \beta^2\right\} E = 0 \quad (1)$$

The transverse electric field is transformed to the local coordinate system by

$$E_{\bar{Y}} = (1 + r/a\cos\phi)^{-1/2} E(r, \phi) e^{-i\beta z} \quad (2)$$

To use perturbation theory to solve eqn. 1, we recognise that the quantity $(\rho/a) \ll 1$, where ρ is the radius of the fibre. Thus $E(r)$ and β^2 can be expanded in an ascending series of (ρ/a) as

$$E = E_0 + \frac{\rho}{a}E_1 + \frac{\rho^2}{a^2}E_2 + \cdots$$

$$\beta^2 = \beta_0^2 + \frac{\rho}{a}\beta_1^2 + \frac{\rho^2}{a^2}\beta_2^2 + \cdots \quad (3)$$

where E_0 and β_0 are the field and the propagation constant in the straight (unperturbed) fibre. Using a Taylor expansion on the second term in eqn. 1, and substituting in eqn. 3 yields a system of simultaneous differential equations for E_0, E_1 and E_2:

$$DE_0 = 0 \quad (4a)$$

$$DE_1 = \beta_1^2 E_0 - 2\frac{r}{\rho}\cos\phi\beta_0^2 E_0 \quad (4b)$$

$$DE_2 = \beta_1^2 E_1 + \beta_2^2 E_0 - 2\frac{r}{\rho}\cos\phi\beta_0^2 E_1 - 2\frac{r}{\rho}\cos\phi\beta_1^2 E_0 + 3\frac{r^2}{\rho^2}\cos^2\phi\beta_0^2 E_0 - \frac{1}{4\rho^2}E_0 \quad (4c)$$

where Df is the wave equation of the unperturbed fibre:

$$Df = \left(\frac{\partial^2}{\partial r^2} + \frac{1}{r}\frac{\partial}{\partial r} + \frac{1}{r^2}\frac{\partial^2}{\partial \phi^2} + (k^2 n^2 - \beta_0^2)\right) f$$

Multiplying eqn. 4a by E_1 and eqn. 4b by E_0, subtracting and integrating over the infinite cross-section, yields the propagation-constnat correction β_1^2:

$$\beta_1^2 = 2\beta_0^2 \int_{A_\infty} (r/\rho)\cos\phi E_0^2\, dA \Big/ \int_{A_\infty} E_0^2\, dA \quad (5)$$

It is seen that $\beta_1^2 = 0$ for any symmetric fibre, hence the lowest-order correction to β_0^2 behaves as $(\rho/a)^2$. Applying a similar operation between eqns. 4a and 4c yields the next higher-order term, β_2^2:

$$\beta_2^2 = 2\beta_0^2 \int_{A_\infty} (r/\rho)\cos\phi E_0 E_1\, dA \Big/ \int_{A_\infty} E_0^2\, dA - 3\beta_0^2 \int_{A_\infty} (r/\rho)^2\cos^2\phi E_0^2\, dA \Big/ \int_{A_\infty} E_0^2\, dA + \frac{1}{4\rho^2} \quad (6)$$

If we use the approximation $\beta_0^2 \simeq k^2 n_{co}^2 = V^2/\rho^2(2\Delta)$, where V is the normalised frequency and k is the free-space wavenumber, then we see from eqn. 4*b* that $E_1 \sim V^2/(2\Delta)E_0 \gg E_0$, and the second and third terms of eqn. 6 can be neglected. The equation for the lowest-order correction to the propagation constant is then given by

$$\beta_2^2 = \frac{2}{\rho^2}\frac{V^2}{2\Delta}\int_{A_\infty} R\cos\phi E_1 E_0\, dA \Big/ \int_{A_\infty} E_0^2\, dA \tag{7}$$

where we have introduced the dimensionless radial coordinate $R = r/\rho$.

We introduce normalised fibre parameters U and W, where $U^2 + W^2 = V^2$ and

$$U = \rho(k^2 n_{co}^2 - \beta_0^2)^{1/2}$$
$$W = \rho(\beta_0^2 - k^2 n_{cl}^2)^{1/2}$$

The refractive-index profile can be written in the form $n^2 = n_{co}^2(1 - 2\Delta f)$, where for the step profile $f = 0$ in the core and $f = 1$ in the cladding. For clad power-law profile $f = R^q$ in the core, where q is a grading parameter, and $f = 1$ in the cladding. The step-profile corresponds to $q = \infty$.

3 Bent step-index slab waveguide

3.1 Solutions to the perturbation equations

Here we consider the effect bending has on the fields of a symmetric slab waveguide, unbounded in the y-direction, as shown in Fig. 2. The field eqns. 4 can then be written

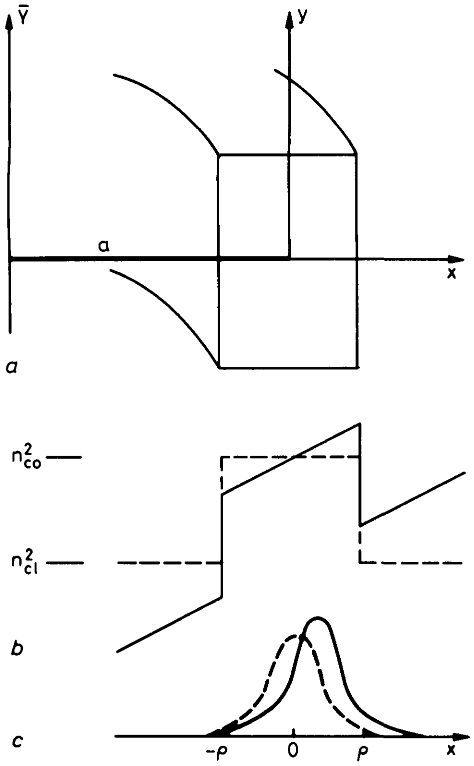

Fig. 2 *Bent slab waveguide*
a Coordinate system
b Effective refractive index due to the bend
c Shift of the field intensity towards the outer core/cladding boundary

as

$$DE_0 = 0$$
$$DE_1 = -\frac{2}{\rho^2}\frac{V^2}{2\Delta} X E_0 \tag{8}$$

where X is the dimensionless coordinate, $X = x/\rho$, and ρ is the half width of the guide. The fields for a step-profile slab waveguide are specified by

$$E_0 = \begin{cases}\cos(UX)/\cos(U) \\ \sin(UX)/\sin(U)\end{cases} \quad 0 < |X| \leq 1$$
$$= \begin{cases}\exp(-W|X|)/\exp(-W) \\ (X/|X|)\exp(-W|X|)/\exp(-W)\end{cases} \quad |X| > 1 \tag{9}$$

for $\begin{cases}\text{even} \\ \text{odd}\end{cases}$ modes.

The method of solution of eqn. 8 is left to Appendix 10. The results agree with those in References 11 and 12.

3.2 Exact solution to the wave equation

As is well known, the effect of the bend on the fields is to shift the field towards the outer core/cladding boundary. This can be shown by rewriting eqn. 1 to first order in (ρ/a) as

$$\left\{\frac{\partial^2}{\partial X^2} + \rho^2(k^2 n_e^2 - \beta^2)\right\}E(X) = 0 \tag{10}$$

where n_e^2 is an effective refractive index which takes into account the bend of the waveguide:

$$n_e^2 = n^2 + 2n_{co}^2\left(\frac{\rho}{a}\right)X \tag{11}$$

The approximation $\beta^2 \simeq k^2 n_{co}^2$ has been used in eqn. 10.

The effective refractive index indicates a shift in the field intensity towards the outer core/cladding boundary, as shown in Fig. 2*b* and 2*c*. As the radius of curvature decreases, the guiding power (the refractive index of the core) of the waveguide shifts away from the centre.

The perturbation solutions are given in Table 1 and illustrated in Fig. 2*c*. They are the so-called 'straight-waveguide solutions' for the effective index of eqn. 11 — the fields in the cladding exponentially decay to zero and never become radiative, regardless of the magnitude of the radius of curvature. However, as Fig. 3 indicates, the fields do become radiative; that is the wave is no longer guided, at some distance x_R from the centre of the core when $\beta = kn_{cl}$.

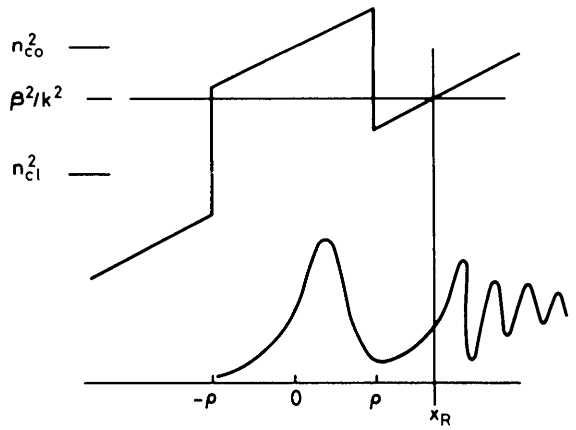

Fig. 3 *Schematic representation of the first mode of eqn. 13*
Normalised radiation point, x_R/ρ, is the point in the cladding where the propagation constant satisfies $\beta = kn_{cl}$ and the field becomes radiative

Eqn. 10 can be solved exactly, remembering that this is a first-order approximation to eqn. 1. Considering a step-

Table 1: Fields of the bent slab waveguide

$$E=\left(1+\left(\frac{\rho}{a}\right)X\right)^{-1/2}\left(E_0+\left(\frac{\rho}{a}\right)E_1\right)$$

E_0	E_1	Region
$\cos(UX)/\cos U$ even	$-\left(\frac{V^2}{2\Delta}\right)\left(\frac{1}{2U}\right)\left\{\sin(UX)\left(X^2-\frac{1}{2U^2}-C_{co}\right)+\cos(UX)\left(\frac{X}{U}\right)\right\}\Big/\cos(U)$	core
$\sin(UX)/\sin U$ odd	$\left(\frac{V^2}{2\Delta}\right)\left(\frac{1}{2U}\right)\left\{\cos(UX)\left(X^2-\frac{1}{2U^2}-C_{co}\right)-\sin(UX)\left(\frac{X}{U}\right)\right\}\Big/\sin(U)$	core
$e^{-W\lvert X\rvert}/e^{-W}$ even	$\left(\frac{V^2}{2\Delta}\right)\left(\frac{1}{2W}\right)\left(\lvert X\rvert X+\frac{X}{W}+\frac{\lvert X\rvert}{X}C_{cl}\right)e^{-W\lvert X\rvert}/e^{-W}$	clad
$\frac{X}{\lvert X\rvert}e^{-W\lvert X\rvert}/e^{-W}$ odd	$\left(\frac{V^2}{2\Delta}\right)\left(\frac{1}{2W}\right)\left(X^2+\frac{\lvert X\rvert}{W}+C_{cl}\right)e^{-W\lvert X\rvert}/e^{-W}$	clad

$$C_{co}=\left(1+\frac{1}{W}\right)^2-\frac{1}{2U^2}\qquad C_{cl}=\left(1+\frac{1}{W}\right)\left(\frac{W}{U^2}-1\right)$$

profile waveguide, we write eqn. 10 as

$$\left\{\frac{\partial^2}{\partial X^2}+U^2+\left(\frac{\rho}{a}\right)\frac{V^2}{\Delta}X\right\}E=0 \quad \text{core}$$
$$\left\{\frac{\partial^2}{\partial X^2}-W^2+\left(\frac{\rho}{a}\right)\frac{V^2}{\Delta}X\right\}E=0 \quad \text{cladding} \tag{12}$$

These equations can be solved in terms of Airy functions, and are given by

$$E=Ai(-z_1)$$
$$E=\kappa_1 Ai(-z_2)+i\kappa_2 Bi(-z_2)$$
$$z_1=(AX+U^2)/A^{2/3} \quad \text{core} \tag{13}$$
$$z_2=(AX-W^2)/A^{2/3} \quad \text{clad}$$

where

$$A=2\left(\frac{\rho}{a}\right)\frac{V^2}{2\Delta},$$

and κ_1 and κ_2 are normalisation constants. The eigenvalues and normalisation constants of eqn. 13 are found by matching the core and cladding fields and their first derivatives at the boundary $X = 1$. Eqn. 13 is shown qualitatively in Fig. 3.

The normalised radiation point, x_R/ρ, is found when the propagation constant $\beta^2/k^2 = W^2/\rho^2k^2 + n_{cl}^2$ is equal to the effective refractive index n_e^2 of eqn. 11:

$$X_R \equiv \frac{x_R}{\rho}=\left(\frac{a}{\rho}\right)\frac{\Delta}{V^2}W^2 \tag{14}$$

Substituting this into the field for the cladding gives $E_{clad} = A_i(0)$.

4 Bent step-index optical fibre

4.1 Fields of the bent fibre

The E_0 fields of the (l, m)-mode, straight circularly symmetric fibre in the 'weakly guiding' approximation are given by

$$E_0=F_l(R)\begin{cases}\cos l\phi & \text{even}\\ \sin l\phi & \text{odd}\end{cases}$$
$$F_l(R)=\begin{cases}J_l(UR)/J_l(U) & \text{core}\\ K_l(WR)/K_l(W) & \text{clad}\end{cases} \tag{15}$$

where J_l and K_l are the usual Bessel functions. Matching these fields and their first derivatives at the fibre boundary $R = 1$ gives the eigenvalue equation

$$U\frac{J_{l+1}(U)}{J_l(U)}=W\frac{K_{l+1}(W)}{K_l(W)} \tag{16}$$

The mth zero of this equation determines the (l, m) mode.

The method of solution of the perturbation eqns. 4 is left to Appendix 10. The fields for the first few modes, with both odd and even symmetry, for the bent step-profile fibre are presented in Table 2. The equation for the bent field for the $l = 0$ mode agrees with the result of References 16 and 18. The method of solution outlined in Appendix 10 can be applied to any mode, for either odd or even symmetry.

The modal fields for the $l = 0$ and $l = 1$ odd and even modes are shown in Fig. 4, where as an example we have chosen a few-mode fibre with $V = 5$ ($\Delta = 0.0035$, $\rho = 4.1$ μm, $\lambda = 0.632$ μm) and fixed bending radius of $a = 1$ cm.

4.2 Change to the propagation constant

The correction to the propagation constant β_2^2 is found by substituting the fields of Table 2 into eqn. 7. The general solution is given in Appendix 10, and the results are summarised in Table 3.

The difference in the propagation constants for the $l = 1$ mode is

$$\delta\beta=\beta_e-\beta_o=\frac{1}{4\rho}\left(\frac{V^2}{2\Delta}\right)^{3/2}B(V)\left(\frac{\rho}{a}\right)^2$$
$$B(V)=\frac{1}{U^2}\left(\frac{1}{W^2}\frac{J_2(U)}{J_0(U)}(W^2-U^2)-\frac{J_1^2(U)}{J_0^2(U)}\right) \tag{17}$$

where subscripts e and o represent the even and odd mode, respectively, and the eigenvalue eqn. 16 has been used. In Fig. 5 we plot the function $B(V)$ against normalised frequency V.

The group delay is specified by $d\beta/d\omega$, and thus in the bent fibre the $l = 1$ mode will separate into linearly polarised odd and even modes, where the separation varies as $(\rho/a)^2$. In Appendix 10 it is shown that only the $l = 1$ mode will split when first-order perturbation terms are used.

The effect of profile variation on the mode splitting can be examined by considering the clad power-law profile, described by the profile given at the end of

Table 2: Electric field of the bent fibre

$$E=\left(1+\left(\frac{\rho}{a}\right)R\cos\phi\right)^{-1/2}\left(E_0+\left(\frac{\rho}{a}\right)E_1\right)$$

Mode	E_0	E_1		Region
$l=0$	$J_0(UR)/J_0(U)$	$f^{0}_{co}(R)\cos\phi$	$f^{0}_{co}=2\left(\frac{V^2}{2\Delta}\right)UR^2\frac{J_1(UR)}{J_0(U)}\left\{\frac{A_0}{R^2}-\frac{1}{4U^2}\right\}$	core
	$K_0(WR)/K_0(W)$	$f^{0}_{cl}(R)\cos\phi$	$f^{0}_{cl}=2\left(\frac{V^2}{2\Delta}\right)WR^2\frac{K_1(WR)}{K_0(W)}\left\{\frac{B_0}{R^2}+\frac{1}{4W^2}\right\}$	clad
$l=1$ odd	$\frac{J_1(UR)}{J_1(U)}\sin\phi$	$f^{odd}_{co}(R)\sin 2\phi$	$f^{odd}_{co}=\left(\frac{V^2}{2\Delta}\right)UR^2\frac{J_2(UR)}{J_1(U)}\left\{\frac{A_1}{R^2}+\frac{1}{4U^2}\frac{J_0(UR)}{J_2(UR)}\right\}$	core
	$\frac{K_1(WR)}{K_1(W)}\sin\phi$	$f^{odd}_{cl}(R)\sin 2\phi$	$f^{odd}_{cl}=\left(\frac{V^2}{2\Delta}\right)WR^2\frac{K_2(WR)}{K_1(W)}\left\{\frac{B_1}{R^2}+\frac{1}{4W^2}\frac{K_0(WR)}{K_2(WR)}\right\}$	clad
$l=1$ even	$\frac{J_1(UR)}{J_1(U)}\cos\phi$	$f^{even}_{co}(R)\cos 2\phi+g^{even}_{co}(R)$ $f^{even}_{co}=f^{odd}_{co}$ $g^{even}_{co}=\left(\frac{V^2}{2\Delta}\right)UR^2\frac{J_0(UR)}{J_1(U)}\left\{\frac{C_1}{R^2}-\frac{1}{4U^2}\frac{J_2(UR)}{J_0(UR)}\right\}$		core
	$\frac{K_1(WR)}{K_1(W)}\cos\phi$	$f^{even}_{cl}(R)\cos 2\phi+g^{even}_{cl}(R)$ $f^{even}_{cl}=f^{odd}_{cl}$ $g^{even}_{cl}=\left(\frac{V^2}{2\Delta}\right)WR^2\frac{K_0(WR)}{K_1(W)}\left\{\frac{D_1}{R^2}+\frac{1}{4W^2}\frac{K_2(WR)}{K_0(WR)}\right\}$		clad

$A_0=\left\{\frac{2}{W}\frac{K_1}{K_0}+1\right\}\Big/4U^2$ $\quad B_0=\left\{\frac{2}{U}\frac{J_1}{J_0}-1\right\}\Big/4W^2$ $\quad C_1=\left\{-\frac{K_2}{K_0}\right\}\Big/4U^2$

$A_1=\left\{\frac{4}{W}\frac{K_0}{K_1}+\frac{K_0}{K_2}\right\}\Big/4U^2$ $\quad B_1=\left\{-\frac{4}{U}\frac{J_0}{J_1}+\frac{J_0}{J_2}\right\}\Big/4W^2$ $\quad D_1=\left\{+\frac{J_2}{J_0}\right\}\Big/4W^2$

$K_l\equiv K_l(W)$ $\quad J_l\equiv J_l(U)$

Table 3: Correction to the propagation constant

Mode	β_2^2
$l=0$	$\left(\frac{V^2}{2\Delta}\right)^2\frac{1}{V^2}\left\{2A_0W^2-\frac{W^2}{6U^2}\left(2-\frac{J_2^2}{J_1^2}\right)+2B_0U^2+\frac{U^2}{6W^2}\left(2+\frac{K_2^2}{K_1^2}\right)\right\}$
$l=1$ odd	$\left(\frac{V^2}{2\Delta}\right)^2\frac{1}{2V^2}\left\{2A_1\left(2-\frac{J_1^2}{J_0J_2}\right)W^2-\frac{1}{6}\frac{W^2}{U^2}\left(2\frac{J_1^2}{J_0J_1}-\frac{J_2}{J_0}\right)\right.$ $\left.+2B_1U^2\left(2-\frac{K_1^2}{K_0K_2}\right)+\frac{1}{6}\frac{U^2}{W^2}\left(2\frac{K_1^2}{K_0K_2}+\frac{K_2}{K_0}\right)\right\}$
$l=1$ even	$\beta_2^2\begin{pmatrix}l=1\\ \text{odd}\end{pmatrix}+\left(\frac{V^2}{2\Delta}\right)^2\frac{1}{V^2}\left\{-2C_1W^2\frac{J_1^2}{J_0J_2}+\frac{1}{2}\frac{W^2}{U^2}\frac{J_2}{J_0}\right.$ $\left.+2D_1U^2\frac{K_1^2}{K_0K_2}+\frac{1}{2}\frac{U^2}{W^2}\frac{K^2}{K_0}\right\}$

Section 2. Fig. 5 shows the variation of the mode splitting as a function of V for two values of q. As V gets large, or q small, the splitting becomes smaller.

Fig. 5 indicates that maximum splitting occurs for the largest profile volume, which is the step profile. The larger the profile volume, the better the guiding power of the fibre. Thus for small profile volumes, or in the case of the clad power-law profile small values of q, the fibre does not guide the higher-order modes as efficiently, and the nondegeneracy of the $l = 1$ modes become less pronounced. This is because the $l = 1$ mode, as compared to the fundamental modes, has most of its intensity near the core/cladding boundary and so its guidance is very sensitive to profile changes. As q becomes small, the intensity peaks of the $l = 1$ mode virtually lie in the cladding and the mode loses its guiding power. Thus the subtle effects of mode splitting decrease as the $l = 1$ mode loses its power to the cladding as the grading of the profile increases.

Near cut-off the propagation constants vary rapidly with respect to V [8], and the rate of change approaches infinity. It is in this region that the difference between the two propagation constants changes sign and becomes very large, as shown in Fig. 5. However, the modes are not strongly guided in this region, and the above discussion concerning the effect of profile variation does not apply.

To experimentally investigate the theoretical mode splitting described by eqn. 17 we propose the use of a stimulated four-photon mixing process [19], in which pump waves excite the odd and even symmetries of the $l = 1$ modes and generate a Stokes and an anti-Stokes wave. The phase-matched condition for this process determines the frequency shift Ω between pump and generated waves. This nonlinear process is easily achieved in fibres for quite low pump intensities.

5 Gaussian approximation to the fields

It is well known that the Gaussian approximation is useful when describing the modal fields of a fibre, and the simple analytic forms of the approximation should offer some insight into the effect on modal characteristics due to bending. Here we present simple analytic forms for the perturbed field E_1, which allow an evaluation of the shift in the intensity peaks, and propagation constant correction β_2^2.

The fields in the straight fibre are specified by the Gaussian approximation of Reference 20, and in Table 4 we give E_0 for the (01), (11) odd and (11) even modes. The spot size R_0 may be determined from a variational procedure [20]. The spot size is not the same for different modes. The perturbation eqns. 4 are easily solved for E_1, and the integrals in eqn. 7 are trivial. The results are summarised in Table 4.

The Gaussian-approximation correction to the propagation constant is the same for the odd and even $l = 1$

modes, and thus no splitting is predicted. While the field of the $l = 0$ mode is a reasonably good approximation, as shown in Fig. 4*a*, the higher-order modes are not well represented. The difference between the exact and approximate value of β_2^2 for the $l = 0$ mode is 17% and 13% at $V = 2.35$ and $V = 5$, respectively. The optimum V is $V = 3.3$, where the percentage difference between exact and approximate values is 5%. Thus the Gaussian

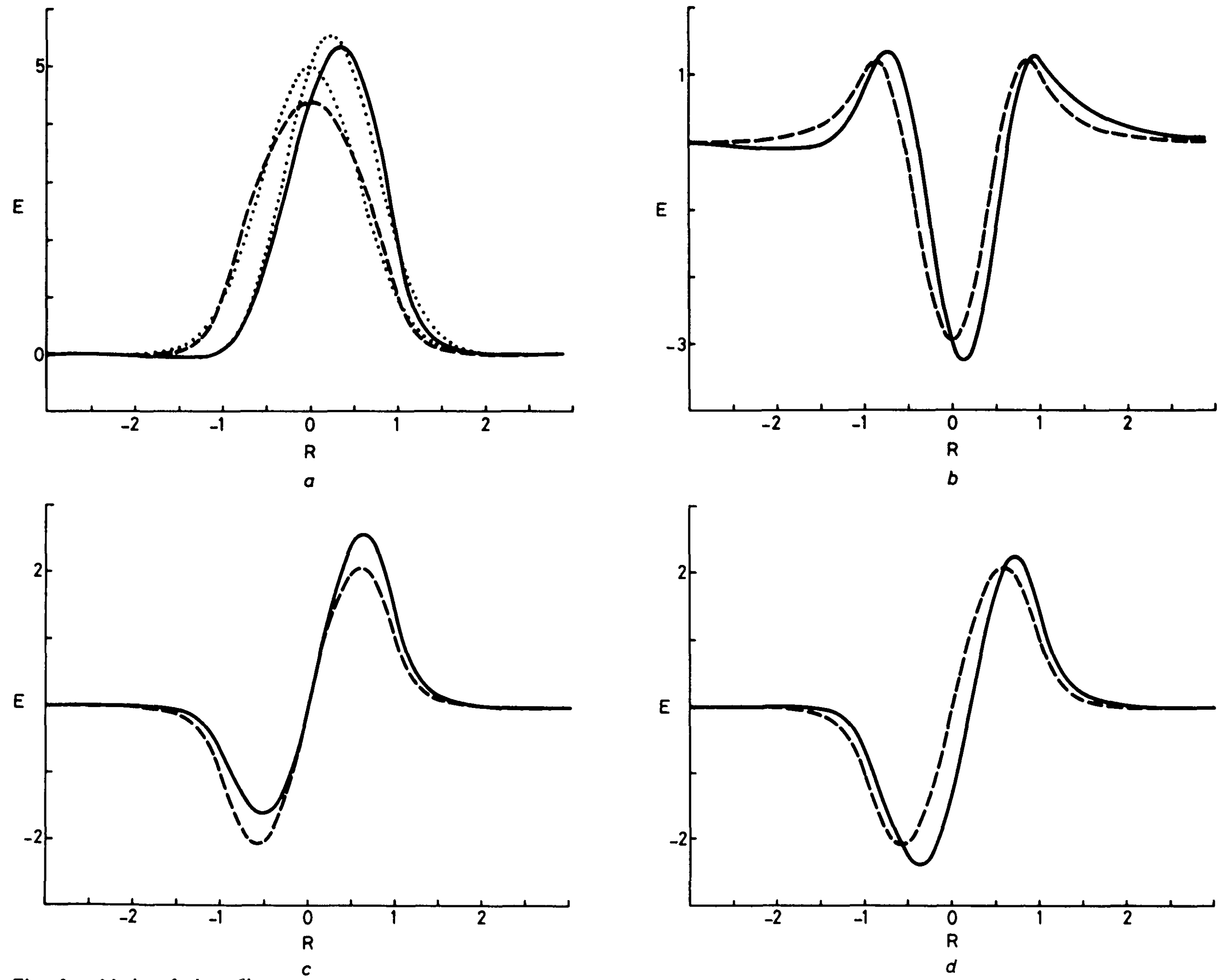

Fig. 4 *Modes of a bent fibre*
a Fundamental (LP01) mode
b LP02 mode
c LP11 odd mode
d LP11 even mode
Characteristics: $\rho = 4.1$ μm, $\Delta = 0.0035$, $\lambda = 0.632$ μm, $V = 5$
– – – – radius of curvature $a = \infty$ (straight fibre)
——— radius of curvature $a = 1$ cm
······· Gaussian approximation where Gaussian field has been normalised to have the same modal power as the exact field in the straight fibre

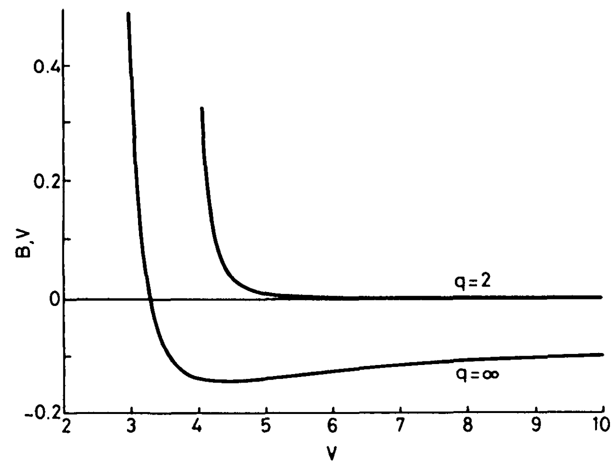

Fig. 5 *Normalised difference in propagation constants for the $l = 1$ odd and even modes for a clad power-law profile against normalised frequency V*
$q = \infty$ is the step profile

approximation offers simple analytic expressions for the modal fields of the bent fibre, particularly the fundamental mode, but is not suited to explaining the subtle effects of mode splitting, described by the propagation-constant corrections.

The shift of the peak intensity of the fundamental-mode field occurs when $\partial E^2/\partial R = 0$ and is given by

$$R_s = \left(\frac{\rho}{a}\right)\left(\frac{V^2}{2\Delta}\right) R_0^4 \cos\phi$$

which agrees with the result of Reference 20.

6 Expansion parameter

The simple forms of the Gaussian approximation allow an investigation of the higher-order solutions of the field equations. The field in the bent fibre can be expressed as

$$E = \sum_{n=0}^{\infty} \left(\frac{\rho}{a}\right)^n E_n$$

Table 4: Gaussian approximation to fields of the bent fibre

Mode	(01)	(11) odd	(11) even
E_0	$e^{-R^2/2R_0^2}$	$\frac{R}{R_0} e^{-R^2/2R_0^2} \sin\phi$	$\frac{R}{R_0} e^{-R^2/2R_0^2} \cos\phi$
E_1	$cR\cos\phi e^{-R^2/2R_0^2}$	$cR\sin\phi\cos\phi \frac{R}{R_0} e^{-R^2/2R_0^2}$	$cR\left(\cos^2\phi - \frac{R_0^2}{R^2}\right)\frac{R}{R_0} e^{-R^2/2R_0^2}$
β_2^2	c^2/ρ^2	c^2/ρ^2	c^2/ρ^2
		$c = \rho^2\beta_0^2 R_0^2 \simeq \frac{V^2}{2\Delta} R_0^2$	

Eqn. 2 can then be expanded so that the differential equation for E_n results, in an analogous manner to the derivation of eqn. 4. Using the Gaussian approximation for the fundamental mode it can be shown that

$$E_n = \frac{1}{n!}(cR\cos\phi)^n E_0 \tag{18}$$

where c and E_0 are given in Table 4. We note that eqn. 18 represents the fundamental ($l = 0$) mode of the bent fibre. It is apparent that the perturbation expansion results in coefficients in powers of $\varepsilon = (\rho/a)c$. This parameter may become quite large, invalidating the perturbation theory, for quite moderate bending radii.

In Fig. 6, c is plotted against V for several values of profile height Δ. If the operating wavelength λ and fibre radius ρ are specified, then the value of c for any fibre can be found from Fig. 6. The minimum bend radius for the perturbation theory to remain valid is then given by $a_{min} = \rho c/\varepsilon_{max}$, where ε_{max} is the expansion parameter, and its value will dictate the accuracy of the perturbation theory. For example, if $\varepsilon \leqslant 0.5$ then for the few-mode fibre of Fig. 4 ($V = 5$) $a_{min} \geqslant 1.5$ cm, and for the same fibre operating at 1.3 μm ($V = 2.35$) $a_{min} \geqslant 0.5$ cm. For values of bend radius smaller than a_{min} the mode characteristics described in this paper will be invalidated.

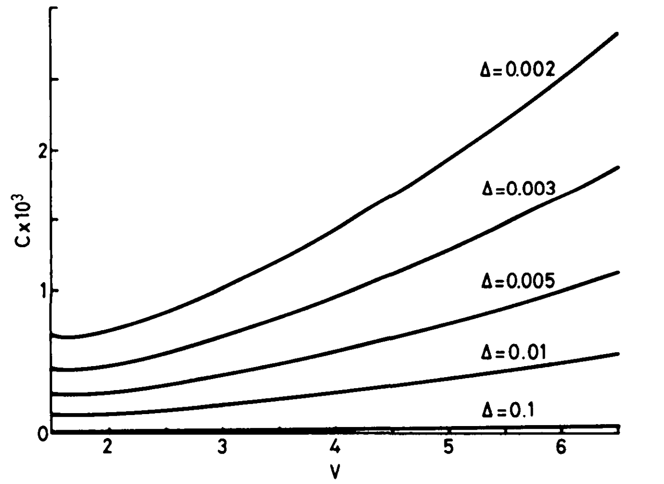

Fig. 6 *Perturbation parameter c against normalised frequency V for a range of profile heights Δ*

7 Discussion

Using first-order perturbation theory, simple analytic expressions for the fields and propagation constants of a bent step-index optical waveguide have been obtained. The bend breaks the symmetry of the waveguide, and the scalar propagation constants of the higher-order modes become nondegenerate. The $l = n$ mode set will become nondegenerate when the nth-order term in the perturbation expansion is included in the analysis. For example, using first-order perturbation theory only the $l = 1$ scalar mode set splits, with a difference in propagation constants given by eqn. 17, whereas to that order the scalar $l \geqslant 2$ mode set remains degenerate.

The perturbation solutions are nonphysical in that the fields in the cladding always decay to zero, regardless of the magnitude of the bend. We have shown, by still using first-order perturbation theory, that solutions can be obtained for the step-index slab waveguide which give the point in the cladding at which the field becomes radiative.

Finally, we have examined the validity of the perturbation theory, and shown that the expansion parameter may become unreasonably large for quite moderate bend radii, i.e. for some multimode fibres bend radii of a few centimeters will invalidate the theory.

8 Acknowledgment

The author thanks Colin Pask for many valuable discussions and comments.

9 References

1 MARCATILI, E.A.J.: 'Bends in optical dielectric guides', *Bell Syst. Tech. J.*, 1969, **48**, pp. 2013–2132
2 KUESTER, E.F., and CHANG, D.C.: 'Surface-wave radiation loss from curved dielectric slabs and fibres', *IEEE J. Quantum Electron.*, 1975, **QE-11**, pp. 903–907
3 WHITE, I.A.: 'Radiation from bends in optical waveguides: The volume-current method', *IEE J. Microwaves, Opt. & Acoust.*, 1979, **3**, pp. 186–188
4 MARCUSE, D.: 'Field deformation and loss caused by curvature of optical fibres', *J. Opt. Soc. Am.*, 1976, **66**, pp. 311–320
5 PETERMAN, K.: 'Theory of microbending loss in monomode fibres with arbitrary refractive index profiles', *Arch. Elektron. & Uebertragungstech.*, 1976, **30**, pp. 337–342
6 PETERMAN, K.: 'Microbending loss in monomode fibres', *Electron. Lett.*, 1976, **12**, pp. 107–109
7 SNYDER, A.W.: 'Asymptotic expressions for eigenfunctions and eigenvalues of a dielectric or optical waveguide', *IEEE Trans.*, 1969, **MTT-17**, pp. 1130–1144
8 GLOGE, D.: 'Weakly-guiding fibres', *Appl. Opt.*, 1971, **10**, pp. 2252–2258
9 SNYDER, A.W., and YOUNG, W.R.: 'Modes of optical waveguides' *J. Opt. Soc. Am.*, 1978, **68**, pp. 297–307
10 GARTH, S.J., and PASK, C.: 'Field shift and birefringence in bent single-mode fibres', *J. Lightwave Technol.*, 1987, **LT-5**
11 KANAKAMI, S., MIYAGI, M., and NISHIDA, S.: 'Bending losses of dielectric slab optical waveguide with double or multiple claddings: theory', *Appl. Opt.*, 1975, **14**, pp. 2588–2597
12 TAKUMA, Y., MIYAGI, M., and KANAKAMI, S.: 'Bent asymmetric dielectric slab waveguides: a detailed analysis', *ibid.*, 1981, **20**, pp. 2291–2298
13 MIYAGI, M., and YIP, G.L.: 'Field deformation and polarization change in a step-index optical fibre due to bending', *Opt. & Quantum Electron.*, 1976, **8**, pp. 335–341
14 SAKAI, J.J., and KIMURA, T.: 'Fields in a curved optical fibre', *IEEE J. Quantum Electron.*, 1981, **QE-17**, pp. 29–34

15 GAMBLING, W.A., MATSUMURA, H., and SAMMUT, R.A.: 'Mode shift at bends in single-mode fibres', *Electron. Lett.*, 1977, **13**, pp. 695–697
16 BAO, Z.W., MIYAGI, M., and KAWAKAMI, S.: 'Measurements of field deformations caused by bends in a single mode optical fibre', *Appl. Opt.*, 1983, **22**, pp. 3678–3680
17 GAMBLING, W.A., MATSUMURA, H., and RAGDALE, C.M.: 'Field deformation in a curved single-mode fibre', *Electron. Lett.*, 1978, **14**, pp. 130–132
18 WRIGHT, J.V.: 'Microbending loss in monomode fibres: Solutions of Peterman's auxiliary function', *Electron. Lett.*, 1983, **19**, pp. 1067–1068
19 STOLEN, R.H.: 'Phase-matched stimulated four-photon mixing in silica-fibre waveguides', *IEEE J. Quantum Electron.*, 1975, **QE-11**, pp. 100–103
20 SNYDER, A.W., and LOVE, J.D.: 'Optical waveguide theory'. (Chapman and Hall, 1983)
21 WATSON, G.N.: 'A treatise on the theory of Bessel functions'. (Cambridge University Press, 1958)

10 Appendix

10.1 Single-layer slab waveguide

For a step-profile single-layer slab waveguide the field in the straight (unperturbed) waveguide is given by eqn. 9. Assuming a solution to eqn. 8 is given by

$$E_1 = \Phi E_0 \tag{19}$$

the resulting first-order differential equation for Φ' is

$$\Phi'' + \Phi'\left(\frac{2E_0'}{E_0}\right) = -2\rho^2\beta_0^2 X \tag{20}$$

This can be solved with the help of integrating factors:

$$\begin{Bmatrix}\cos^2(UX)\\ \sin^2(UX)\end{Bmatrix} \qquad e^{-2W|X|}$$

for the $\left\{{\text{even} \atop \text{odd}}\right\}$ modes in the core and in the cladding region. The solutions are given in Table 1 where the matching constants are determined by matching Φ_{co} and Φ_{cl} and their first derivatives at the boundary $X = 1$, and using the eigenvalue equations $U \tan U = W$ for the even mode, and $U \cot U = -W$ for the odd mode [20].

10.2 Circularly symmetric fibre

The field in the straight (unperturbed) fibre is

$$E_0 = F_l(R)\begin{Bmatrix}\cos l\phi\\ \sin l\phi\end{Bmatrix} \tag{21}$$

where $F_l(R)$ is given by eqn. 15 and the solution for the first-order correction to the field is of the form

$$E_1 = f_l(R)\begin{Bmatrix}\cos(l+1)\phi\\ \sin(l+1)\phi\end{Bmatrix} + g_l(R)\begin{Bmatrix}\cos(l-1)\phi\\ \sin(l-1)\phi\end{Bmatrix} \tag{22}$$

for $\left\{{\text{even} \atop \text{odd}}\right\}$ modes. Upon substitution into eqn. 4, the resulting differential equations for $f(R)$ and $g(R)$ are

$$\begin{aligned} f'' + \frac{1}{R}f' + \gamma^2 f - \frac{(l+1)^2}{R^2}f &= -\rho^2\beta_0^2 RF_l(R)\\ g'' + \frac{1}{R}g' + \gamma^2 g - \frac{(l-1)^2}{R^2}g &= -\rho^2\beta_0^2 RF_l(R)\end{aligned} \tag{23}$$

where $\gamma^2 = \rho^2(k^2n^2 - \beta_0^2) = +U^2$ for the core, and $= -W^2$ for the cladding region of a step-profile fibre. The homogeneous solutions to the above equations are

$$\begin{aligned} f_h &= \begin{cases}\bar{A}_l J_{l+1}(UR) & \text{core}\\ \bar{B}_l K_{l+1}(WR) & \text{clad}\end{cases}\\ g_h &= \begin{cases}\bar{C}_l J_{l-1}(UR) & \text{core}\\ \bar{B}_l K_{l-1}(WR) & \text{clad}\end{cases}\end{aligned} \tag{24}$$

A particular solution can be found by assuming $f_p = p_f f_h$ and $g_p = p_g g_h$ resulting in a first-order differential equation for p'

$$p_f'' + p_f'\left(\frac{2f_h'}{f_h} + \frac{1}{R}\right) = -\rho^2\beta_0^2 RF_l/f_h \tag{25}$$

A similar equation results for p_g. Eqn. 25 can be solved with the integrals in Appendix 10.5 and with integrating factors

$$RJ_{l+1}^2(UR) \qquad RK_{l+1}^2(WR) \quad \text{for } p_f$$

and

$$RJ_{l-1}^2(UR) \qquad RK_{l-1}^2(WR) \quad \text{for } p_g$$

for the core and cladding regions, respectively. The solution to eqns. 23 is

$$f_l = f_h(1 + p_f) \qquad g_l = g_h(1 + p_g)$$

and can be written as

$$\begin{aligned} f_l^{co}(R) &= \rho^2\beta_0^2 U\frac{J_{l+1}(UR)}{J_l(U)} \times\left(A_l + \frac{R^2}{4U^2}\frac{J_{l-1}(UR)}{J_{l+1}(UR)}\right) \quad \text{core}\\ f_l^{cl}(R) &= \rho^2\beta_0^2 W\frac{K_{l+1}(WR)}{K_l(W)} \times\left(B_l + \frac{R^2}{4W^2}\frac{K_{l-1}(WR)}{K_{l+1}(WR)}\right) \quad \text{clad}\\ g_l^{co}(R) &= \rho^2\beta_0^2 U\frac{J_{l-1}(UR)}{J_l(U)} \times\left(C_l - \frac{R^2}{4U^2}\frac{J_{l+1}(UR)}{J_{l-1}(UR)}\right) \quad \text{core}\\ g_l^{cl}(R) &= \rho^2\beta_0^2 W\frac{K_{l-1}(WR)}{K_l(W)} \times\left(D_l + \frac{R^2}{4W^2}\frac{K_{l+1}(WR)}{K_{l-1}(WR)}\right) \quad \text{clad}\end{aligned} \tag{26}$$

where the matching constant A_l is related to $\bar{A}_l$ of eqn. 24 by

$$A_l = \bar{A}_l J_l(U)/\rho^2\beta_0^2 U$$

and similarly for the other constants.

The constants are determined by matching the functions $f_l^{co}(R)$, $g_l^{co}(R)$ and $f_l^{cl}(R)$, $g_l^{cl}(R)$ and their first derivatives at the fibre boundary $R = 1$, and using the eigenvalue eqn. 14:

$$\begin{aligned} A_l &= \left(\frac{2}{W}(l+1)\frac{K_{l-1}(W)}{K_l(W)} + \frac{K_{l-1}(W)}{K_{l+1}(W)}\right)\frac{1}{4U^2}\\ B_l &= \left(-\frac{2}{U}(l+1)\frac{J_{l-1}(U)}{J_l(U)} + \frac{J_{l-1}(U)}{J_{l+1}(U)}\right)\frac{1}{4W^2}\\ C_l &= \left(\frac{2}{W}(l-1)\frac{K_{l+1}(W)}{K_l(W)} - \frac{K_{l+1}(W)}{K_{l-1}(W)}\right)\frac{1}{4U^2}\\ D_l &= \left(-\frac{2}{U}(l-1)\frac{J_{l+1}(U)}{J_l(U)} + \frac{J_{l+1}(U)}{J_{l-1}(U)}\right)\frac{1}{4W^2}\end{aligned} \tag{27}$$

and $A_0 = -C_0$, $B_0 = D_0$.

10.3 Correction if the propagation constant
Substituting eqns. 21 and 22 into eqn. 7 yields

$$\delta\beta_0 = \frac{2\beta_0^2}{\chi_0}\int_0^\infty F_0(R)f_0(R)R^2\,dR \qquad l = 0$$

$$\delta\beta_1 = \frac{\beta_0^2}{\chi_1}\left[\int_0^\infty F_1(R)f_1(R)R^2\,dR + 2\int_0^\infty F_1(R)g_1(R)R^2\,dR\begin{Bmatrix}1\\0\end{Bmatrix}\right] \quad \begin{Bmatrix}\text{even}\\ \text{odd}\end{Bmatrix} l = 1$$

$$\delta\beta_l = \frac{\beta_0^2}{\chi_l}\int_0^\infty F_l(R)(f_l(R) + g_l(R))R^2\,dR \qquad l > 1$$

where $\delta\beta \equiv \beta_2^2$ and

$$\chi_l = \int_0^\infty F_l^2(R)R\,dR = \frac{V^2}{2U^2}\frac{K_{l-1}(W)K_{l+1}(W)}{K_l^2(W)}$$

With the help of the integrals in Appendix 10.5, the results presented in Table 3 are obtained. The difference in the even and odd propagation constants of the higher-order modes are

$$\beta_e^2 - \beta_o^2 = \delta\beta_e - \delta\beta_o = \begin{cases} \dfrac{2\beta_0^2}{\chi_1}\displaystyle\int_0^\infty F_1(R)g_1(R)R^2\,dR & l = 1 \\ 0 & l > 1 \end{cases}$$

Using the approximation $\beta_e^2 - \beta_o^2 \simeq 2\beta_0(\beta_e - \beta_o)$ we obtain eqn. 17 for the $l = 1$ case.

10.4 Stability of LP modes on a bent fibre
The criterion that modes are linearly polarised on optical fibres is [9]

$$\Lambda = (\beta_e - \beta_o)/(\beta_1 - \beta_2) \gg 1 \tag{28}$$

where β_e and β_o are the even and odd propagation constants of the bent scalar equation and β_1 and β_2 are the exact modes (i.e. scalar modes plus polarisation corrections) of the circularly symmetric straight fibre. $\beta_e - \beta_o$ is given by eqn. 17 and $\beta_1 - \beta_2$ is found in Reference 9. Substituting into eqn. 28 we have

$$\Lambda \sim \left(\frac{V^2}{2\Delta}\right)^3\left(\frac{\rho}{a}\right)^2 \gg 1 \tag{29}$$

For the few-mode fibre of Fig. 4 ($V = 5$, $\rho = 4.1$ μm, $\Delta = 0.0035$) the modes will be linearly polarised for curvature radius $a < 80$ cm.

10.5 Some Bessel functions integrals

$$\int xZ_l^2\,dx = \tfrac{1}{2}x^2(Z_l^2 - Z_{l-1}Z_{l+1}) \tag{30}$$

$$\int x^2 Z_l Z_{l\pm1}\,dx = \pm\tfrac{1}{2}x^2Z_l^2 + (l \mp 1)\int xZ_l^2\,dx \tag{31}$$

$$3\int x^3Z_l^2\,dx = 2(l^2 - 1)\int xZ_l^2\,dx - x^2(l-1)Z_l(Z_l + xZ_{l+1}) + \tfrac{1}{2}x^4(Z_l^2 + Z_{l+1}^2) \tag{32}$$

$$\int x^4 Z_l Z_{l\pm1}\,dx = \mp\tfrac{1}{2}x^4Z_l^2 + (l \pm 2)\int x^3Z_l^2\,dx \tag{33}$$

$$\int \frac{x}{Z_{l\pm1}^2}(lZ_l^2 - (l \pm 1)Z_{l-1}Z_{l+1})\,dx = \mp x^2\frac{Z_{l\mp1}}{Z_{l\pm1}} \tag{35}$$

where $Z_l = J_l(x) = K_l(-ix)/i^{l+1}$.
Integral eqns. 30 and 32 obtained from Schafheitlin's reduction formula [21].